Design Comparison of NdFeB and Ferrite Radial Flux Surface Permanent Magnet Coaxial Magnetic Gears

Matthew Johnson
IEEE Member
mjohnson11@tamu.edu

Matthew C. Gardner
IEEE Student Member
gardner1100@tamu.edu

Hamid A. Toliyat
IEEE Fellow
toliyat@tamu.edu

Advanced Electric Machines & Power Electronics Lab
Texas A&M University
College Station, TX 77843

***Abstract*— Magnetic gears promise the benefits of mechanical gears with added advantages from contactless power transfer. Although most literature focuses on minimizing the size of magnetic gears, their material costs must also be reduced to achieve economic feasibility. This work compares the active material costs of NdFeB and ferrite radial flux coaxial magnetic gears with surface permanent magnets through a parametric 2D and 3D finite element analysis (FEA) study. Differences in optimal design trends such as pole count and magnet thicknesses are illustrated for the two materials. The results demonstrate that, for most historical price rate scenarios, NdFeB gear designs are capable of achieving lower active material costs than ferrite gear designs, and they are always capable of achieving much higher torque densities. Based on the selected design constraints, relative to a nominal ferrite cost of $10/kg, NdFeB must cost more than $90/kg before ferrite is cost competitive. However, ferrite gears can achieve higher efficiencies than NdFeB gears, especially at high speeds, and generally emit less axial leakage flux. Additionally, contour plots are provided to show the impact of material price rate variation on the cost break points.**

Keywords*— *cost; end effects; ferrite; finite element analysis; magnetic gear; NdFeB; optimization; radial flux; torque density.

I. Introduction

Recently, magnetic gears have drawn significant interest as an alternative to their mechanical counterparts [1]-[4]. Instead of achieving the gearing effect through mechanical contact, magnetic gears rely on modulated interaction between flux generated by magnets on the rotors. This provides a plethora of potential advantages, such as inherent overload protection, improved reliability, and physical isolation between shafts. Furthermore, various magnetically geared machine topologies integrate a magnetic gear with a conventional permanent magnet (PM) motor or generator to produce a single device with the compactness of mechanically geared systems and the reliability of traditional direct drive machines [5], [6]. As a result, magnetic gears have attracted interest for use in several applications including wind turbines [7], wave energy generation [8], and electric vehicles [6].

Most literature on magnetic gears focuses on maximizing their torque density to make them competitive in size with mechanical gears [9], [10], but minimizing cost is also essential for the technology to achieve commercial success. One of the first decisions in the design of a magnetic gear is the selection of the magnet material. In an effort to reduce magnet costs, some literature suggests using weaker, but less expensive ferrite magnets instead of NdFeB magnets [8], [11]. This tactic is further motivated by the volatility of rare earth magnet prices, as shown in Fig. 1 [12], which makes many manufacturers leery of relying on rare earth magnets. Some studies have evaluated the torque density of NdFeB and ferrite magnetic gears on the basis of limited parametric sweeps [9] or the permanent magnet costs for the same single design with different magnet materials [11]. However, while thorough magnet material cost studies have been performed for conventional machines [13], [14], there is no known comprehensive comparison for individually optimized magnetic gears using the different materials and illustrating their divergent impacts on trends. Because the ferrite and NdFeB magnets result in different optimum designs, it is crucial to consider the best gear for each material to perform a proper comparison for a given objective. Much of this study is presented in [15], but information on axial leakage flux issues and the variation of losses with speed is added in this version.

II. Design Study Methodology

This work analyzes the coaxial radial flux magnetic gear topology with surface mounted permanent magnets shown in Fig. 2 and examines the impact of using ferrite or NdFeB magnets on various design trends. In particular, tradeoffs between active material cost minimization and torque density maximization are characterized to highlight the effects of the magnet materials. As indicated by the material properties listed in Table I, a relatively strong grade of ferrite was selected for use in the comparison analysis.

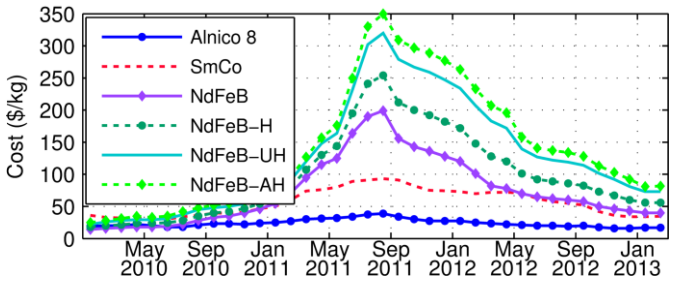

Fig. 1. Rare Earth Permanent Magnet Cost Trends [12]

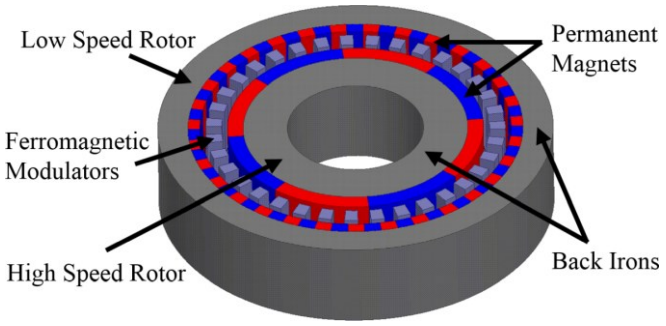

Fig. 2. Coaxial Radial Flux Magnetic Gear with Surface Permanent Magnets

For this study, the gear's inner, low pole count structure serves as the high speed rotor (HSR), the outer, high pole count structure is used as the low speed rotor (LSR), and the intermediate modulator assembly is stationary. Alternatively, the high pole count assembly could be held stationary and the modulators allowed to rotate in its place, but, while this would increase the magnitude of the gear ratio of each design by 1 and provide a corresponding increase in stall torque, it would not change any optimization patterns. The number of modulators (Q_M) is related to the number of pole pairs on the HSR (P_{HS}) and on the LSR (P_{LS}) according to the established expression in (1), and the resulting gear ratio, which relates the speeds of the HSR (ω_{HS}) and the LSR (ω_{LS}), is given by (2).

$$Q_M = P_{HS} + P_{LS} \tag{1}$$

$$\text{Gear Ratio} = \frac{\omega_{HS}}{\omega_{LS}} = \frac{-P_{LS}}{P_{HS}} \tag{2}$$

This study primarily focuses on the active material cost and torque density and neglects factors such as structural material (housing, bearings, etc.), manufacturing considerations (such as the impact of varying the radius on achievable air gap sizes), and assembly costs. In particular, the cost of each gear design is evaluated based on the assumption that its constituent materials, listed in Table I, each have a fixed price per unit mass, independent of the necessary component sizes and shapes. This is a simplification with respect to the reality that smaller, more complex sizes and shapes could increase the effective material prices and manufacturing costs. Thus, for the purposes of this analysis, the cost of a given design can be calculated by determining the requisite amounts of steel (used to form the rotor back irons and modulators) and permanent magnet material (either NdFeB or ferrite) and applying (3). The costs in Table I are used to demonstrate design trends and optimization patterns. However, because these patterns will vary slightly with the cost of the materials and because the dramatic volatility of NdFeB prices illustrated in Fig. 1 is a primary motivation for this investigation, the study also provides an analysis of the impact of NdFeB, ferrite, and steel cost rate variations on optimal costs and torque densities.

$$\text{Cost} = (\text{PM Mass})\cdot(\text{PM Rate}) + (\text{Steel Mass})\cdot(\text{Steel Rate}) \tag{3}$$

TABLE I. CHARACTERISTICS OF MAGNETIC GEAR MATERIALS

Material	Density	B_r	Cost Rate
N42 NdFeB	7400 kg/m^3	1.3 T	\$50/kg
Hitachi NMF-12F Ferrite	4800 kg/m^3	0.46 T	\$10/kg
M47 Steel (26 Gauge)	7870 kg/m^3	N/A	\$3/kg

To characterize the different design trends for both NdFeB and ferrite magnetic gears, several critical geometric gear parameters were swept over the ranges of values specified in Table II. Because there are strong interdependencies between the effects of different dimensions, the values of certain variables were coupled through derived parameters, which are included in Table II. First, the radial thickness of the LSR magnets, T_{LSPM}, is determined by the radial thickness of the HSR magnets, T_{HSPM}, and a ratio, k_{PM}, as indicated in (4). This relationship is employed because the LSR has more magnetic poles than the HSR, which leads to increased flux leakage, so it is cost effective to keep the LSR magnets thinner than the HSR magnets. Thus, k_{PM} is swept over a range of values not exceeding 1. The second derived parameter, G_r, represents the approximate (nearest integer) desired gear ratio, and it is used, along with P_{HS}, to drive P_{LS}, as described in (5). This approach keeps the number of modulators even, which results in symmetrical cancellation of the net forces on each rotor. Additionally, this approach maintains a relatively high least common multiple (LCM) between P_{HS} and P_{LS}, which reduces the gear's torque ripple [7].

$$T_{LSPM} = T_{HSPM} \cdot k_{PM} \tag{4}$$

$$P_{LS} = \begin{cases} G_r \cdot P_{HS} + 1 & \text{for } (G_r + 1)\cdot P_{HS} \text{ odd} \\ G_r \cdot P_{HS} + 2 & \text{for } (G_r + 1)\cdot P_{HS} \text{ even} \end{cases} \tag{5}$$

In addition to the design parameters specified in Table II, all permanent magnet pole arcs were set equal to the corresponding pole pitches, as shown in Fig. 2, resulting in 100% angular fill factors for each magnet pole. All modulator pole arcs were set equal to half of the corresponding modulator pole pitches, as shown in Fig. 2, resulting in equally distributed modulator pieces and modulator slots.

TABLE II. PARAMETRIC DESIGN STUDY RANGES

Name	Description	Values	Units
G_r	Nearest integer gear ratio	4, 8, 16	
P_{HS}	HSR pole pairs		
	For $G_r = 4$	3, 4, 5, … 18	
	For $G_r = 8$	3, 4, 5, … 13	
	For $G_r = 16$	3, 4, 5, … 8	
R_{Out}	Gear's active outer radius	100, 125, 150	mm
T_{HSBI}	HSR back iron thickness	5, 10, 20	mm
T_{HSPM}	HSR magnet thickness	3, 5, 7, 9, 11, 13	mm
T_{AG}	Air gap thickness	1	mm
T_{Mods}	Modulator thickness	8, 11, 14	mm
k_{PM}	LSR magnet thickness ratio	0.5, 0.75, 1	
T_{LSBI}	LSR back iron thickness	5, 10, 20	mm

All 48,114 designs specified by the combinations of parameter values in Table II were evaluated for both ferrite and NdFeB gears using static 2D finite element analysis (FEA) simulations at the stall torque alignment. Additionally, because several studies report significant discrepancies between the magnetic gear performance results predicted by 2D and 3D FEA simulations, due to axial leakage flux, more accurate 3D simulation models were used in this investigation where necessary (further explanation is provided in the following section). Although there is already a good analysis of the key trends related to these 3D effects [16], this study provides additional insight into their relative significance for a wider array of designs. Based on these 2D and 3D simulations, each gear design case was linearly scaled to the stack length required to achieve a stall torque of 250 N·m on the LSR. For each case, this stack length and the cross-sectional design were used to determine the gear volume and constituent material masses for torque density and active material cost calculations. In practice, a magnetic gear must be operated below its stall torque, but this will not change optimization trends.

Two additional considerations, demagnetization and magnetic flux containment, were addressed by analyzing the results and removing designs from the population set if they did not meet certain criteria with respect to these issues. Demagnetization was handled based on the static simulation results by evaluating the percentage of the magnet bodies operating at flux densities below the knee point of their demagnetization curves at 20 °C. Although this does not comprehensively quantify the full extent of the demagnetization that will occur during operation, nor does it address the temperature dependent nature of this phenomenon, it does indicate which designs are most susceptible to demagnetization. To that end, designs with more than 1% of the magnet volume operating below the knee point were removed from the population. Adequate magnetic flux containment was ensured by eliminating designs with an RMS flux density greater than 10 mT on either the circular path 1 mm inside of the HSR back iron or the circular path 1 mm outside of the LSR back iron. This filtration process also served as one means of determining the acceptable back iron thicknesses for a given design. The other primary performance issues affected by the back iron sizing are the gear's cost, torque density, and efficiency. Cost and torque density were addressed simply by calculating these values for each design and selecting the best results that were not eliminated due to demagnetization or magnetic containment issues. Efficiency was considered for the most cost effective and torque dense designs by performing 2D transient simulations to evaluate their full load losses at an LSR operating speed of 100 rpm.

III. Results

The analysis of the simulation results is separated into five sections. The first set of graphs shown in Figs. 3-7 is based on the fixed cost rates provided in Table I and contains large sets of design points to simply illustrate general performance capabilities and trends, such as cost, torque density, mass, 3D effects, and efficiency, for various design subsets. The second set of graphs shown in Figs. 8-12 is also based on the fixed component cost rates provided in Table I and depicts detailed optimization patterns with respect to key design parameters for both NdFeB and ferrite gears. The third set of plots in Figs. 13-15 demonstrates the impact of material cost rate variations on the design optimization results. Fourth, Fig. 16 illustrates the effects of speed on electromagnetic losses for a few optimal designs. Finally, Figs. 17-18 show the axial leakage flux characteristics of different gear designs, which are a major factor in sizing the housing for a magnetic gear.

A. Overview of Results

Fig. 3 displays the active material costs, torque densities, and active masses of the most cost effective NdFeB and ferrite gear designs based on 2D FEA results, excluding those that suffered from poor magnetic containment or susceptibility to demagnetization. The data in these plots verifies the well-known facts that NdFeB magnetic gears can achieve significantly higher torque densities and much lower active masses than ferrite magnetic gears. Additionally, the graphs illustrate the previously unestablished conclusion that optimally designed NdFeB magnetic gears also have lower active material costs than optimally designed ferrite gears (based on the cost rates in Table I). Furthermore, these results indicate that the NdFeB gear designs with the lowest active material costs do not have the highest torque densities and vice versa. The highest torque density for any NdFeB design is 200 $kN{\cdot}m/m^3$ with an active material cost of $110 and an active mass of 4.1 kg. However, the most cost effective NdFeB design has an active material cost of $65 with a torque density of only 93 $kN{\cdot}m/m^3$ and an active mass of 4.7 kg. This divergence in optimization trends is primarily due to the fact that maximizing torque density requires using thicker magnets, but minimizing the active material cost of NdFeB designs requires using thinner permanent magnets. The same divergence is also present to a lesser extent in the ferrite gear data set. The most compact ferrite design achieves a torque density of 26 $kN{\cdot}m/m^3$ at an active material cost of $153 and an active mass of 24 kg, while the most cost effective ferrite gear design has an active material cost of $121 at a torque density of 21 $kN{\cdot}m/m^3$ and an active mass of 23 kg. The difference between the optimization extremes is smaller for the ferrite data set because the ratio of the ferrite to steel costs is smaller than the ratio of NdFeB to steel costs, and thus the overall cost is not simply minimized by using the thinnest acceptable ferrite magnets. If the cost of structural material were considered, it would affect the larger designs more than the smaller designs. Thus, the highest torque density NdFeB designs would have the lowest structural costs, while the lowest active material cost NdFeB designs would have slightly higher structural costs, and the ferrite designs would have much higher structural costs.

As noted earlier, magnetic gear designs can suffer from significant end effects due to axially escaping leakage flux not accounted for in 2D models. To address this issue, a subset of the most cost effective and torque dense NdFeB designs were re-simulated using 3D models at the stack lengths predicted by the 2D models and the corresponding active material cost, torque density, and active mass results are shown in Fig. 4, along with the 2D ferrite design results. As indicated by their lower torque densities, the ferrite designs require much longer

stack lengths than the NdFeB designs and, as result, they experience less significant 3D effects. Thus, 3D ferrite gear simulations were only conducted for the optimal designs represented in Figs. 10-18. Due to the impact of the 3D effects, the maximum NdFeB design torque density decreased from 200 kN·m/m^3 to 143 kN·m/m^3 and the minimum NdFeB design active material cost increased from \$65 to \$74, both of which are still superior to the corresponding optimum ferrite gear designs. Note that if the target torque rating was increased and the same radii were used, the required stack lengths would increase, which would reduce the impact of 3D effects [16].

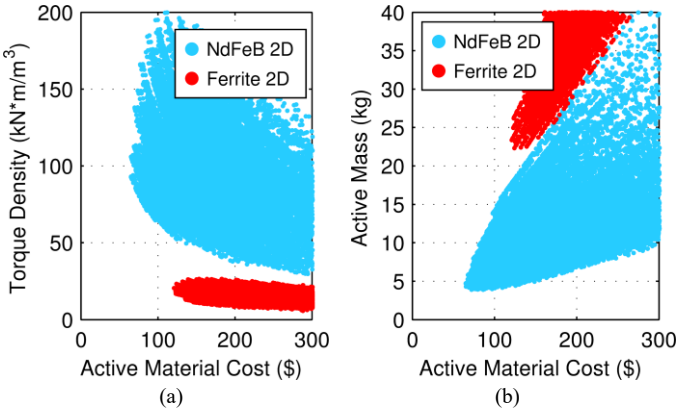

Fig. 3. Active Material Cost, (a) Torque Density, and (b) Active Mass for the Best Gear Designs Based on 2D Simulations

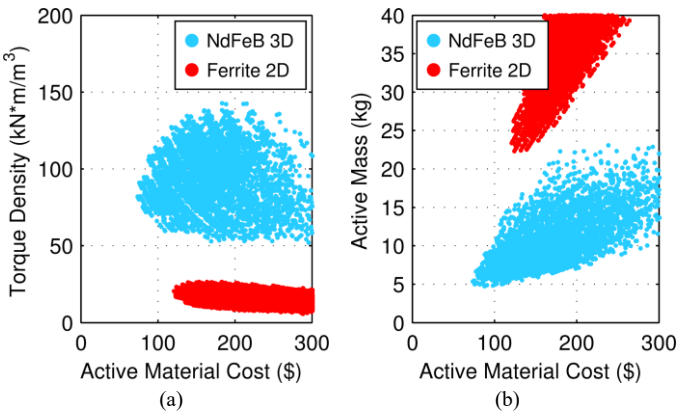

Fig. 4. Active Material Cost, (a) Torque Density, and (b) Active Mass for the Best Gear Designs Based on 3D NdFeB and 2D Ferrite Simulations

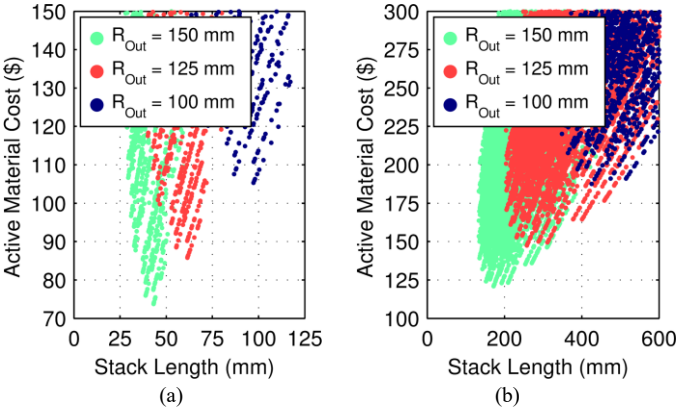

Fig. 5. Relationship between Stack Length, Active Material Cost, and Outer Radius for (a) 3D NdFeB and (b) 2D Ferrite Magnetic Gear Simulations

Figs. 5(a) and 5(b) show the relationship between stack length, active material cost, and outer radius for 3D NdFeB and 2D ferrite magnetic gear simulations. As the outer radius increases, the stack lengths and active material costs of the best designs decrease (although practical designs would likely require larger air gaps at larger radial design points, which would slightly blunt this trend). As indicated by Fig. 5(a), this trend remains true, albeit slightly less significant, even when 3D effects are considered. A comparison of Figs. 5(a) and 5(b) demonstrates that the optimal ferrite gear designs require significantly longer stack lengths than the optimal NdFeB gear designs at the same radius. As noted earlier, these longer stack lengths reduce the impact of 3D effects on the ferrite designs.

Fig. 6 demonstrates the relative impact of 3D effects on NdFeB gear designs with different form factors. As illustrated by the data in Fig. 6, for a fixed torque rating, optimally designed gears with a larger outer radius, and thus a shorter stack length, tend to suffer a more significant reduction in torque, as compared to their 2D model projections. However, despite this consideration, the larger outer radius designs still generally achieve the lowest active material costs.

Fig. 7 shows Pareto optimal fronts for the simulated efficiencies and active material costs. These efficiencies only include the electromagnetic losses (eddy losses in the magnets and core losses in the steel) for operation at the LSR stall torque and an LSR speed of 100 rpm. The losses are determined from 2D transient simulations and linearly scaled to the necessary stack lengths. For the NdFeB designs, the necessary stack lengths are determined by 3D static simulations; however, for the ferrite designs, the necessary stack lengths are determined by 2D static simulations. In both cases, the lower gear ratios achieve higher efficiencies due in part to the fact that the HSR rotates faster for higher gear ratios, which increases the electromagnetic frequencies present in the gear and leads to higher losses. There is also a tradeoff between cost and efficiency, which is primarily related to the selection of pole pair counts and back iron thicknesses. Additionally, despite being larger, the ferrite designs can generally achieve higher efficiencies than the NdFeB designs because the ferrite designs have lower flux densities, which lead to lower steel core loss densities, and because ferrite's resistivity eliminates magnet eddy current losses. A more detailed analysis of the variation of the different gear loss components with speed is provided for a subset of optimal gear designs in a later section of the study.

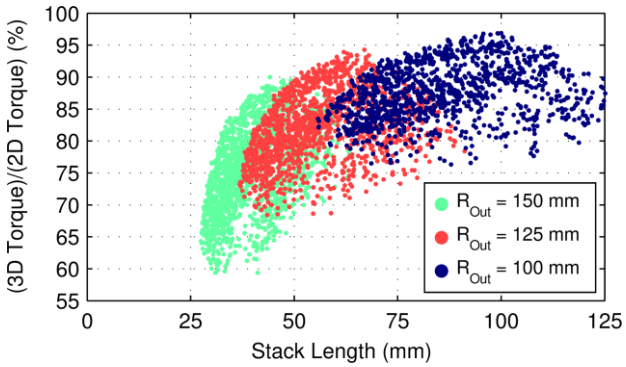

Fig. 6. Impact of Outer Radius on 3D Effects for NdFeB Gear Designs at Different Stack Lengths

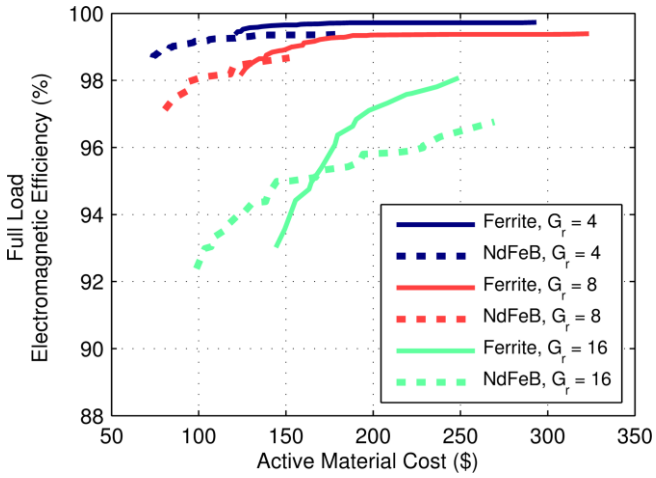

Fig. 7. Pareto Optimal Fronts for NdFeB and Ferrite Gear Designs with Different Gear Ratios

B. *Design Optimization Trends*

In order to demonstrate important design trends and tradeoffs, the effects of several of the design parameters are considered for designs using NdFeB magnets and designs using ferrite magnets at each of the different gear ratios. One key source of the differences in optimization trends for NdFeB and ferrite designs is the difference in the percentage of the active material cost associated directly with the magnet material as indicated in Fig. 8. Trends are evaluated for the NdFeB designs using both 2D and 3D simulation results and for the ferrite designs using 3D simulation results. Fig. 9 provides a legend describing the significance of each of the curves in Figs. 10-12, which demonstrate the impact of different design parameters.

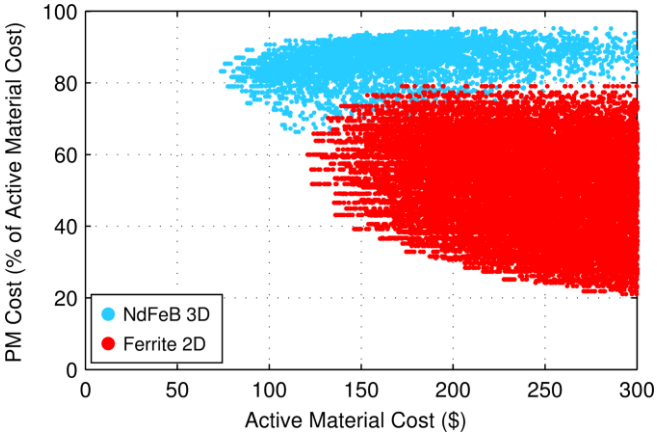

Fig. 8. Percentage of Total Active Material Cost from Magnet Material for NdFeB and Ferrite Designs

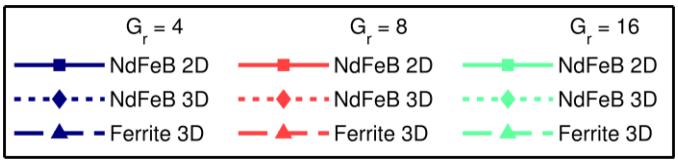

Fig. 9. Legend for Design Optimization Trend Plots in Figs. 10-12

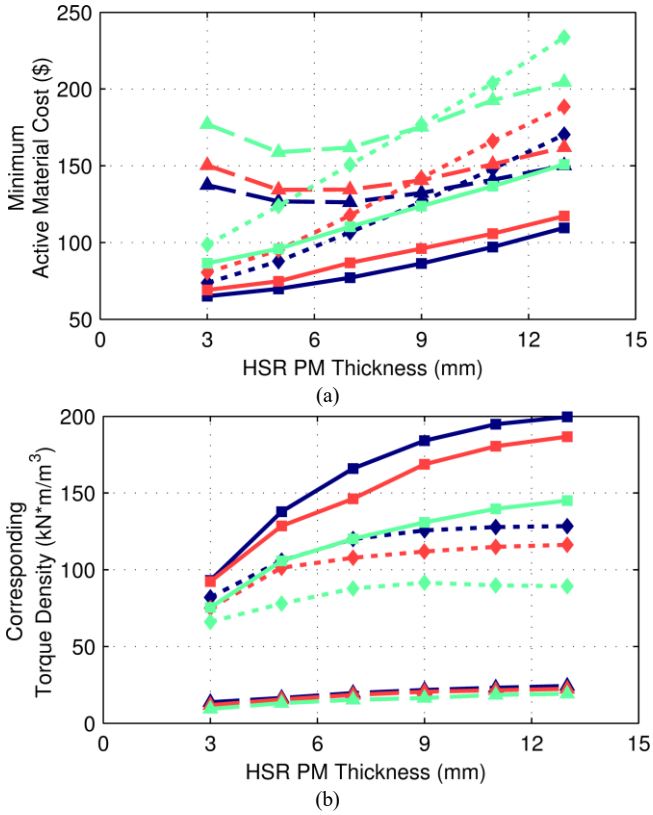

Fig. 10. Impact of HSR Magnet Thickness on (a) the Minimum Active Material Cost and (b) the Corresponding Torque Density

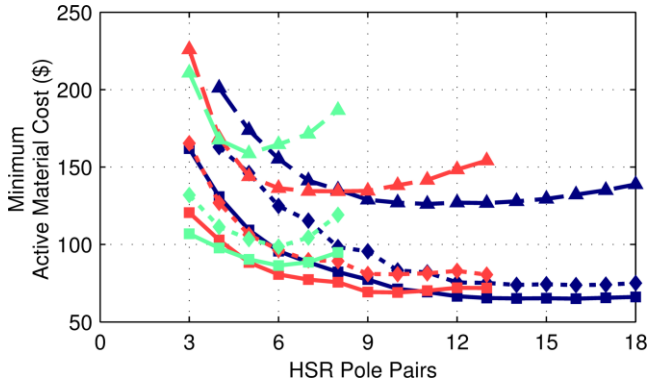

Fig. 11. Impact of HSR Pole Pairs on the Minimum Active Material Cost

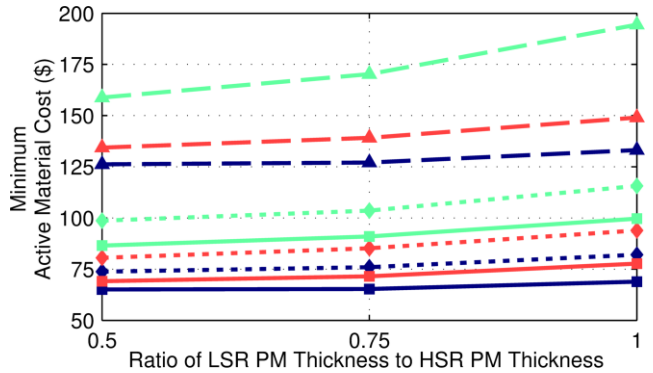

Fig. 12. Impact of the LSR Magnet Thickness Ratio on the Minimum Active Material Cost

Fig. 10(a) illustrates the minimum active material costs that can be achieved with HSR magnets of various thicknesses, and Fig. 10(b) provides the corresponding torque densities of these same minimum cost designs. Fig. 10(a) indicates that the minimum material cost for the NdFeB designs of each gear ratio can be achieved by using the thinnest magnets allowed in the simulation sweep. However, the minimum cost ferrite designs are achieved with thicker magnets. Because the magnet thickness contributes to the effective air gap, increasing the magnet thickness provides diminishing torque returns. Due to the relatively high cost of NdFeB magnets, the optimal NdFeB designs use magnet material almost as efficiently as possible, resulting in relatively thin magnets. However, the cost of iron is more significant in the ferrite designs, as shown in Fig. 8, creating a more significant tradeoff between magnet usage and steel usage. This leads to the optimal ferrite designs having thicker magnets than the optimal NdFeB designs. Fig. 10(b) shows that the torque density of the optimal designs increases with the magnet thickness. However, the 3D simulations reveal less of an increase in torque density than the 2D simulations because the end-effects penalty increases as the increased magnet thickness decreases the stack length.

Fig. 11 shows the effects of varying the HSR pole pair count on the minimum material cost. Higher gear ratios favor lower HSR pole pair counts than lower gear ratios because the gear ratio affects the tradeoff between optimizing the HSR and LSR pole pair counts. Additionally, ferrite designs tend to favor lower HSR pole pair counts than NdFeB designs because the thicker magnets favored by ferrite increase the effective air gap and, thus, the leakage flux per pole. Decreasing the number of poles counteracts this increase in leakage flux.

Fig. 12 illustrates the effect of varying k_{PM}, the ratio of the LSR magnet thickness to the HSR magnet thickness. Because the higher number of poles on the LSR leads to more leakage flux on the LSR, it is cost effective to concentrate most of the magnet material on the HSR. As the gear ratio increases, the difference between the number of LSR and HSR poles increases, leading to a greater improvement achieved by reducing k_{PM}. However, in addition to the practical limitations on producing extremely thin magnets for the LSR, decreasing k_{PM} too far can increase the LSR magnets' susceptibility to demagnetization by the HSR magnets.

C. *Impact of Material Cost Rate Variation*

The previous graphs and analysis are all based on the fixed costs provided in Table I; however, all of the materials, especially NdFeB, have some cost variability, which will impact the optimum designs and minimum achievable active material costs. Figs. 13 and 14 characterize the impact of this variation in NdFeB and ferrite price rates on the minimum costs of the different designs, based on 3D simulation results. Fig. 13 shows the impact of NdFeB price variation on the minimum active material costs of the NdFeB designs relative to the fixed minimum costs of ferrite designs at the nominal ferrite price rate of $10/kg. Fig. 14 shows the impact of ferrite price variation on the minimum active material costs of the ferrite designs relative to the fixed minimum costs of NdFeB designs at the nominal NdFeB price rate of $50/kg. This data shows that, for surface mounted radial flux magnetic gears, relatively high NdFeB prices or low ferrite prices are required before ferrite gears become cost competitive. Under the assumed constraints, relative to the fixed minimum active material costs of the ferrite designs based on a ferrite cost of $10/kg, NdFeB designs with a gear ratio of ~4 require NdFeB to cost at least $93/kg before ferrite is cost competitive, while designs with gear ratios of ~8 and ~16 require NdFeB rates of $92/kg and $91/kg, respectively. Alternatively, relative to the fixed minimum active material costs of the NdFeB designs based on a cost of $50/kg for NdFeB, ferrite designs with a gear ratio of ~4 require ferrite to cost at most $3.3/kg for ferrite to be cost competitive, while designs with gear ratios of ~8 and ~16 require a rate of $3.5/kg or lower. Regardless of active material cost, NdFeB designs are still significantly smaller.

Figs. 13 and 14 describe the impact of magnet material prices on the minimum achievable active material costs for the two sets of magnetic gear designs; however, Fig. 8 reveals that, while the active material costs of NdFeB designs are dominated by the cost of the magnets themselves, the cost of the steel is a non-negligible component of the ferrite gear costs. Thus, a range of costs for all three materials, are considered for a gear ratio of ~4 in the analysis provided in Fig. 15, based on 3D simulation results.

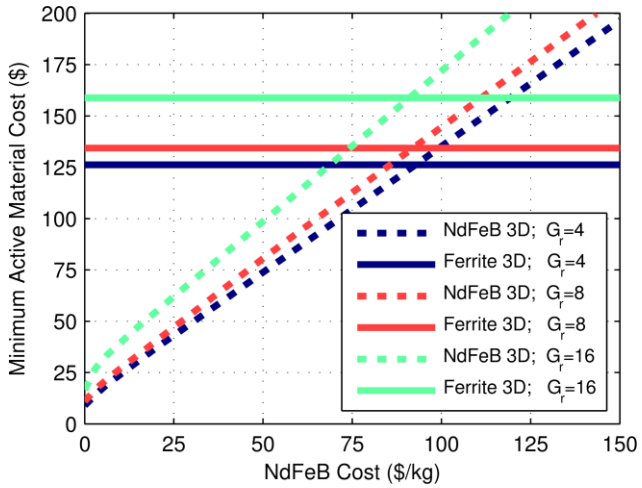

Fig. 13. Impact of NdFeB Cost Variation on Minimum Active Material Cost

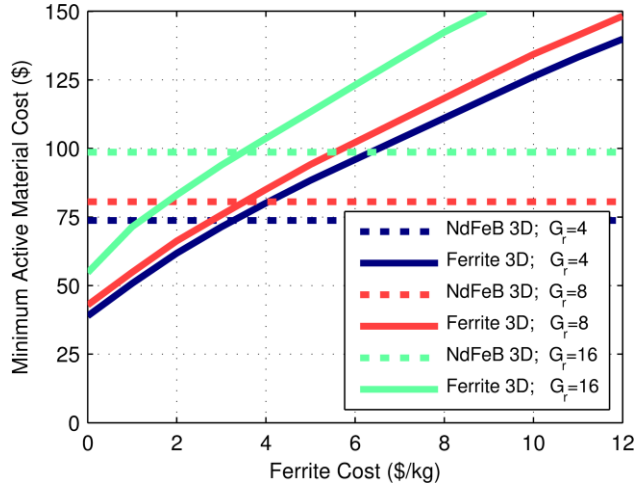

Fig. 14. Impact of Ferrite Cost Variation on Minimum Active Material Cost

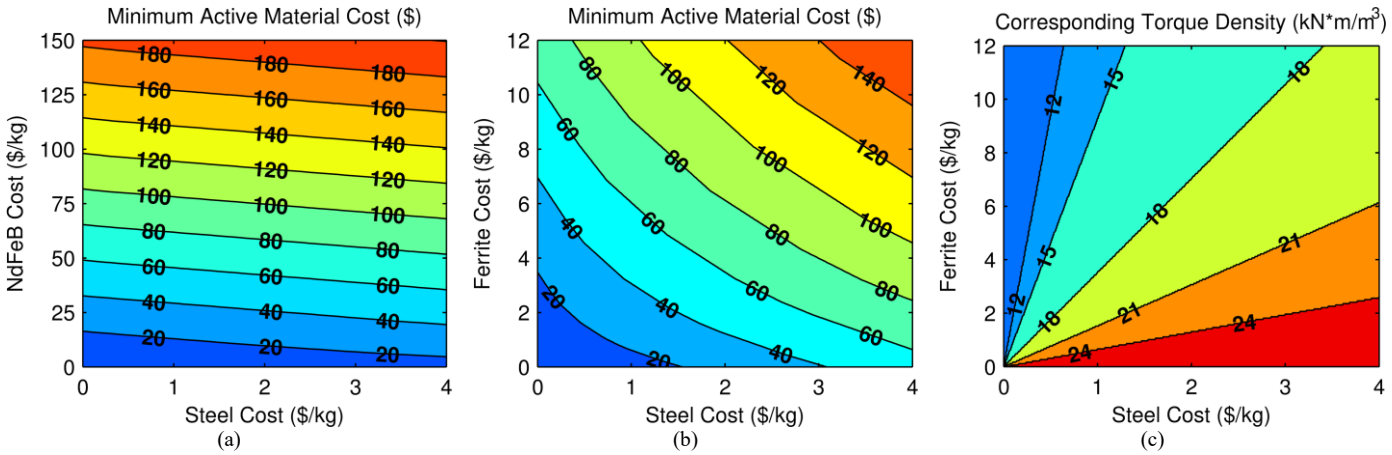

Fig. 15. Effect of Steel and Magnet Costs on (a) Minimum Active Material Cost of NdFeB Designs, (b) Minimum Active Material Cost of Ferrite Designs, and (c) the Corresponding Torque Density of the Minimum Active Material Cost Ferrite Designs with $G_r = 4$

Fig. 15(a) shows the impact of the steel and NdFeB price rates on the minimum achievable active material cost for the NdFeB designs, where the different colors and contour lines indicate the variation in this minimum cost. Similarly, Fig. 15(b) shows the impact of the steel and ferrite price rates on the minimum achievable active material cost for the ferrite designs. Fig. 15(c) illustrates the corresponding torque densities of these same minimum active material cost ferrite designs whose costs are characterized in Fig. 15(b). The trends in Figs. 13-15 display some curvature as prices vary, indicating that the optimal design changes as the material cost rates vary. As the ratio of magnet price to steel price increases, the optimal design increasingly favors thinner, more effectively utilized magnets, decreasing the torque density of the minimum active material cost design, as illustrated in Fig. 15(c).

These results demonstrate that, for most reasonable combinations of NdFeB, ferrite, and steel cost rates, the increased energy density of NdFeB relative to ferrite offsets its higher cost per unit mass, making it the most cost effective magnet material to use in this magnetic gear topology.

D. Variation of Electromagnetic Losses with Speed

While NdFeB gears offer higher torque densities and lower active material costs (for most historical price scenarios), Fig. 7 suggests that ferrite gears can achieve slightly higher electromagnetic efficiencies. However, the results in Fig. 7 are only based on a single LSR operating speed of 100 rpm. For a more thorough loss analysis, the minimum active material cost (based on the rates in Table I) and maximum torque density NdFeB and ferrite gear designs from the 3D parametric design set were selected for 2D transient simulations at LSR speeds ranging from 50 rpm to 500 rpm. Table III summarizes these optimal designs, and Fig. 16 illustrates the variation of their no load electromagnetic loss components with operating speed. (While magnetic gear losses vary slightly with load, they are primarily dependent on operating speed [17].)

The data in Fig. 16 demonstrates that the difference in electromagnetic losses between the NdFeB gears and the ferrite gears increases with speed (note the differences in vertical axis scales for the various graphs in Fig. 16). This is primarily due to the different resistivities of the magnet materials. NdFeB magnets have a low resistivity, so they experience significant eddy current losses which increase quadratically with speed. However, the ferrite magnets' high resistivity prevents appreciable eddy current losses, so the only significant electromagnetic losses in the ferrite gears are the core losses in the modulators and the LSR back iron. Thus, the ferrite gears' small efficiency advantages at lower speeds become more pronounced at higher speeds. Additionally, the minimum active material cost designs tend to have higher losses than the maximum torque density designs, largely due to the use of higher pole counts, which leads to higher electromagnetic frequency flux harmonics. These differences in losses impact both the efficiencies of the gears and how much heat is generated. Regardless of magnet material, most gears experience minimal losses in the HSR back iron because the high pole count LSR magnet flux travels along shorter paths and does not penetrate the HSR back iron as deeply as the low pole count HSR magnet flux penetrates the LSR back iron.

TABLE III. OPTIMAL GEAR DESIGN PARAMETERS AND PERFORMANCES

Parameter	Maximum Torque Density		Minimum Active Material Cost	
	NdFeB	Ferrite	NdFeB	Ferrite
Gear Ratio	4.14:1	4.25:1	4.13:1	4.09:1
HSR Pole Pairs	7	8	16	11
LSR Pole Pairs	29	34	66	45
Outer Radius (mm)	100	150	150	150
HSR Back Iron Thickness (mm)	10	5	5	5
HSR Magnet Thickness (mm)	11	13	3	7
Air Gap Thickness (mm)	1	1	1	1
Modulator Thickness (mm)	8	8	8	8
LSR Magnet Thickness (mm)	5.5	9.75	1.5	3.5
LSR Back Iron Thickness (mm)	5	5	5	5
Stack Length (mm)	55.8	145.1	43.1	179.7
Active Material Cost ($)	183.4	166.3	73.8	126.2
Torque Density (kN·m/m^3)	142.7	24.4	82.0	19.7
Active Mass (kg)	7.5	25.7	5.3	24.4
HSR Pk-Pk Torque Ripple (N·m)	0.41	0.57	0.20	0.32
LSR Pk-Pk Torque Ripple (N·m)	0.18	0.17	0.27	0.16

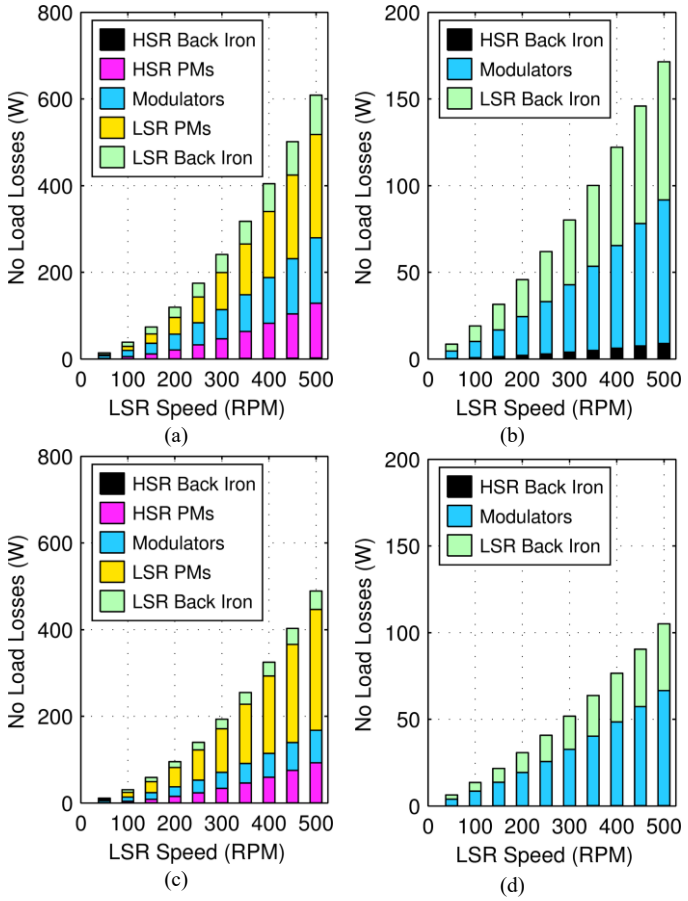

Fig. 16. Simulated Variation of No Load Electromagnetic Loss Components with Speed for the Minimum Active Material Cost (a) NdFeB and (b) Ferrite Gears and the Maximum Torque Density (c) NdFeB and (d) Ferrite Gears

E. Axial Leakage Flux

While the majority of this study neglects structural considerations (except for the elimination of designs with poor radial leakage flux containment), axial leakage flux is a critical magneto-mechanical design consideration which affects both a gear's magnetic performance and its housing design. Gears with high axial leakage flux not only exhibit lower stall torques than the values predicted by 2D FEA simulations, but they can also experience significant eddy current losses in surrounding structural material if the housing design does not include an adequate non-conducting axial buffer. This issue has plagued multiple prior magnetic gear prototypes and contributed to their experimental efficiencies falling well short of their theoretically predicted efficiencies [3], [18].

Fig. 17 depicts the variation of the maximum (across all designs simulated in 3D) RMS leakage flux density 10 mm axially beyond the end of the modulators for different HSR magnet thickness and HSR pole pair combinations in the parametric NdFeB gear design set. Thicker magnets result in stronger opposing MMFs (from the magnets on the two rotors) and larger effective air gaps, which leads to higher axial leakage flux. Lower pole counts also result in more significant axial leakage flux because the flux paths are inherently longer, so the axially leaking flux travels further from the ends of the gear into the surrounding environment.

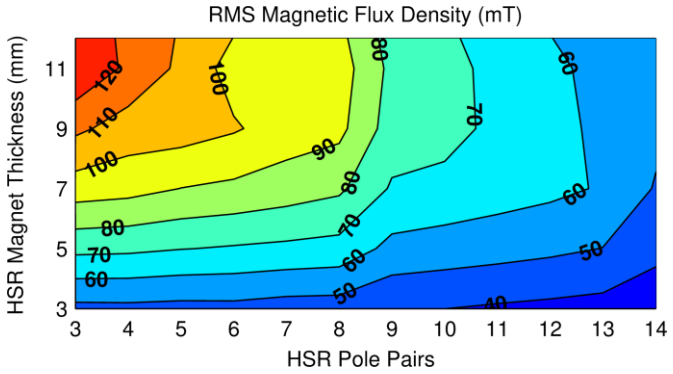

Fig. 17. Variation of the Maximum RMS Leakage Flux Density 10 mm Axially Beyond the Modulators with HSR Magnet Thickness and HSR Pole Pair Count for the Parametric 3D NdFeB Gear Simulations

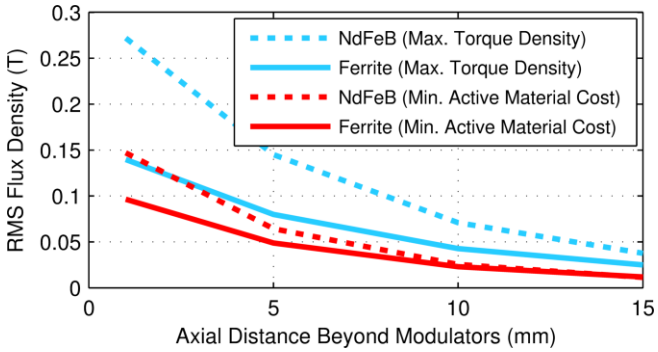

Fig. 18. Variation of the RMS Leakage Flux Density with Axial Distance Beyond the Modulators for the Optimal Gear Designs

Fig. 18 shows the decline in the leakage flux density with axial distance beyond the end of the modulators for the optimal gear designs described in Table III. The data indicates that the maximum torque density designs experience higher axial leakage flux than the minimum active material cost designs because the maximum torque density designs use thicker magnets and lower pole counts. Additionally, the optimal NdFeB gear designs have higher axial leakage flux than the corresponding optimum ferrite gear designs, despite the fact that the ferrite gear designs use longer pole arcs and thicker magnets. This is because the NdFeB magnets are much stronger MMF sources than the ferrite magnets. These results indicate that the non-conducting buffer space required to accommodate the axial leakage flux at both axial ends of the gear is generally larger for the NdFeB designs than it is for the ferrite designs. Additionally, the NdFeB designs generally have shorter active stack lengths than the ferrite designs, so the percentage increases in total effective stack length caused by the axial buffer space will be significantly larger for the NdFeB designs. This consideration could mitigate some of the NdFeB gear torque density and mass advantages, once the inactive housing volume and material are included in the calculations.

IV. Conclusion

Both NdFeB and ferrite radial flux coaxial magnetic gears with surface mounted permanent magnets were parametrically evaluated using 2D and 3D FEA to demonstrate various design trends and performance capabilities with the two different

magnet materials. The results demonstrate that, under the assumed cost scenario of Table I, the optimal NdFeB designs are significantly more cost-effective than the optimal ferrite designs. Under the assumed design constraints, relative to the nominal ferrite cost of $10/kg, a gear ratio of ~4 requires NdFeB to cost at least $93/kg before ferrite is cost competitive, while designs with gear ratios of ~8 and ~16 require NdFeB rates of $92/kg and $91/kg, respectively. Alternatively, relative to the nominal NdFeB cost of $50/kg, a ferrite design with a gear ratio of ~4 requires ferrite to cost at most $3.3/kg for ferrite to be cost competitive, while designs with gear ratios of ~8 and ~16 require a ferrite rate of $3.5/kg.

Additionally, the minimum active material cost was evaluated for NdFeB and ferrite gear designs across a range of combinations of different magnet material and steel cost rates to illustrate the minimum active material costs that could be achieved for each cost scenario. This analysis demonstrated that for most historical price combination scenarios, NdFeB gear designs are still capable of achieving lower active material costs than ferrite gear designs. Furthermore, the results in Fig. 15 indicate that the prices of ferrite magnetic gear designs are significantly more dependent on the price of magnetic steel, as compared to the prices of NdFeB designs. Ferrite designs become increasingly cost-competitive at lower steel prices. Thus, the ratio of all three material cost rates is crucial for determining the best permanent magnetic material to use for a given application. Additionally, the ratio of the material cost rates significantly impacts the optimal design parameters for ferrite magnetic gears. In all cases, regardless of material cost rates, the optimal NdFeB designs achieve significantly lower sizes and masses than the optimal ferrite designs. In addition to being generally undesirable, the higher size and mass of the ferrite designs will incur some additional cost penalties, such as increased housing material expenses, in various applications. However, the ferrite designs are able to achieve higher efficiencies than the NdFeB designs, especially at higher speeds. Furthermore, the lower pole counts and smaller volumes of the maximum torque density designs tend to result in slightly higher efficiencies than those achieved by the minimum active material cost designs. Finally, a gear's axial leakage flux can create significant losses in the surrounding inactive material if not accounted for when sizing the housing. Both low pole counts and thick magnets result in increased axial flux leakage; additionally, axial flux leakage tends to be more severe for the NdFeB designs than for the ferrite designs.

Based on these observations, it is evident that NdFeB magnets are generally preferable for use in radial flux coaxial magnetic gears with surface mounted permanent magnets. Flux focusing topologies have been proposed for ferrite, due to their ability to increase the air gap flux density, but these topologies suffer from increased complexity, poor magnetic containment, and increased susceptibility to demagnetization. However, these topologies could disproportionately improve the performance of ferrite designs relative to NdFeB designs. For simplicity, flux focusing gears were not considered in this analysis. Future studies will evaluate the relative effectiveness of NdFeB and ferrite flux focusing magnetic gear designs to determine how the different topology impacts design and performance trends.

ACKNOWLEDGMENT

The authors would like to thank ANSYS for their generous support of the EMPE lab through the provision of FEA software.

REFERENCES

[1] K. Atallah and D. Howe, "A novel high-performance magnetic gear," *IEEE Trans. Magn.*, vol. 37, no. 4, pp. 2844–2846, Jul. 2001.

[2] N.W. Frank and H. A. Toliyat, "Analysis of the concentric planetary magnetic gear with strengthened stator and interior permanent magnet inner rotor," *IEEE Trans. Ind. Appl.*, vol. 47, no. 4, pp. 1652-1660, July/Aug. 2011.

[3] P. O. Rasmussen, T. O. Anderson, F. T. Jorgensen, and O. Nielsen, "Development of a High Performance Magnetic Gear," *IEEE Trans. Ind. Appl.*, vol. 41, no. 3, pp. 764-770, May/June 2005.

[4] P. M. Tlali, R.-J. Wang, and S. Gerber, "Magnetic gear technologies: A review," *Proc. Int. Conf. Elect. Mach*., 2014, pp. 544–550.

[5] M. Johnson, M. C. Gardner, and H. A. Toliyat, "Design and Analysis of an Axial Flux Magnetically Geared Generator," *IEEE Trans. Ind. Appl.*, vol. 53, no. 1, pp. 97-105, Jan./Feb. 2017.

[6] T. V. Frandsen, L. Mathe, N. I. Berg, R. K. Holm, T. N. Matzen, P. O. Rasmussen, and K. K. Jensen, "Motor integrated permanent magnet gear in a battery electrical vehicle," *IEEE Trans. Ind. Appl.*, vol. 51, no. 2, pp. 1516–1525, Mar./Apr. 2015.

[7] N. W. Frank and H. A. Toliyat, "Gearing ratios of a magnetic gear for wind turbines," *Proc. IEEE Int. Elect. Mach. Drives Conf.*, 2009, pp. 1224–1230.

[8] K. K. Uppalapati, J. Z. Bird, D. Jia, J. Garner, and A. Zhou, "Performance of a magnetic gear using ferrite magnets for low speed ocean power generation," *Proc. IEEE Energy Convers. Congr. Expo.*, 2012, pp. 3348–3355.

[9] K. K. Uppalapati, J. Z. Bird, J. Wright, J. Pitchard, M. Calvin, and W. Williams, "A magnetic gearbox with an active region torque density of 239Nm/L," *Proc. IEEE Energy Convers. Congr. Expo.*, 2014, pp. 1422-1428.

[10] M. Johnson, M. C. Gardner and H. A. Toliyat, "Analysis of axial field magnetic gears with Halbach arrays," *Proc. IEEE Int. Elect. Mach. Drives Conf.*, 2015, pp 108-114.

[11] M. Chen, K. T. Chau, W. Li, and C. Liu, "Cost-effectiveness comparison of coaxial magnetic gears with different magnet materials," *IEEE Trans. Magn.*, vol. 50, no. 2, pp. 821–824, Feb. 2014.

[12] R. Wolf, "Recent History, Current Events, and the Future of Rare Earth and Ferrite Magnets," *Asian Metal Rare Earth Summit*, 2013.

[13] G. Bramerdorfer, S. Silber, G. Weidenholzer, and W. Amrhein, "Comprehensive cost optimization study of high-efficiency brushless synchronous machines," *Proc. IEEE Int. Elect. Mach. Drives Conf.*, 2013, pp. 1126–1131.

[14] P. Zhang, G. Y. Sizov, D. M. Ionel, and N. A. O. Demerdash, "Establishing the relative merits of interior and spoke-type permanent magnet machines with ferrite or NdFeB through systematic design optimization," *IEEE Trans. Ind. Appl.*, vol. 51, no. 4, pp. 2940-2948, July/Aug. 2015.

[15] M. Johnson, M. C. Gardner, and H. A. Toliyat, "Design Comparison of NdFeB and Ferrite Radial Flux Magnetic Gears," *Proc. IEEE Energy Convers. Congr. and Expo.*, 2016, pp. 1-8.

[16] S. Gerber and R-J. Wang, "Analysis of the end-effects in magnetic gears and magnetically geared machines," *Proc. IEEE Int. Conf. Elect. Mach.*, 2014, pp. 396-402.

[17] G. Jungmayr, J. Loeffler, B. Winter, F. Jeske and W. Amrhein, "Magnetic Gear: Radial Force, Cogging Torque, Skewing, and Optimization," *IEEE Trans. Ind. Appl.*, vol. 52, no. 5, pp. 3822-3830, Sept./Oct. 2016.

[18] S. Gerber and R. J. Wang, "Evaluation of a prototype magnetic gear," in *Proc. IEEE Int. Conf. Ind. Technol.*, 2013, pp. 319-324.